



OPEN

## Improved evaluation of left ventricular hypertrophy using the spatial QRS-T angle by electrocardiography

Maren Maanja<sup>1</sup>, Todd T. Schlegel<sup>1,2</sup>, Rebecca Kozor<sup>3,4</sup>, Ljuba Bacharova<sup>5,6</sup>, Timothy C. Wong<sup>7</sup>, Erik B. Schelbert<sup>7</sup> & Martin Ugander<sup>1,4</sup>✉

Electrocardiographic (ECG) signs of left ventricular hypertrophy (LVH) lack sensitivity. The aim was to identify LVH based on an abnormal spatial peaks QRS-T angle, evaluate its diagnostic performance compared to conventional ECG criteria for LVH, and its prognostic performance. This was an observational study with four cohorts with a QRS duration < 120 ms. Based on healthy volunteers (n = 921), an abnormal spatial peaks QRS-T angle was defined as  $\geq 40^\circ$  for females and  $\geq 55^\circ$  for males. In other healthy volunteers (n = 461), the specificity of the QRS-T angle to detect LVH was 96% (females) and 98% (males). In patients with at least moderate LVH by cardiac imaging (n = 225), the QRS-T angle had a higher sensitivity than conventional ECG criteria (93–97% vs 13–56%,  $p < 0.001$  for all). In clinical consecutive patients (n = 783), of those who did not have any LVH, 238/556 (43%) had an abnormal QRS-T angle. There was an association with hospitalization for heart failure or all-cause death in univariable and multivariable analysis. An abnormal QRS-T angle rarely occurred in healthy volunteers, was a mainstay of moderate or greater LVH, was common in clinical patients without LVH but with cardiac co-morbidities, and associated with outcomes.

Left ventricular (LV) hypertrophy (LVH) is a hallmark of cardiac end-organ damage often related to diabetes<sup>1</sup>, hypertension<sup>2</sup>, and obesity<sup>3</sup>. It is also associated with poor cardiovascular outcomes<sup>4</sup>. LVH is defined as an increase in LV mass and is typically diagnosed by non-invasive cardiac imaging such as echocardiography or cardiovascular magnetic resonance (CMR) imaging<sup>5</sup>. However, the increase in LV size is also a substrate for electrical remodeling<sup>6</sup>, and here the ECG provides unique information.

ECG diagnosis of LVH is typically based on increased QRS complex amplitudes, which have a low sensitivity and high or varying specificity<sup>7</sup>. The electrical remodeling in LVH is complex and affects cardiomyocytes as well as the extracellular matrix<sup>8</sup>, and extends beyond changes in QRS amplitudes. Notably, both electrical and anatomical changes attributed to LVH convey independent prognostic information<sup>9</sup>. Taken together, these findings raise several important and related issues. First, the diagnostic performance of ECG criteria for detecting anatomical changes associated with LVH is limited, and this is likely related to the inherent differences between anatomy and electrophysiology. Second, and consequently, it has been suggested that a term such as left ventricular electrical remodeling (LVER) might be more appropriate than LVH when referring to ECG changes<sup>5,10</sup>. Thus, it may be more important to define electrical changes as a deviation from normal ECG values measured in healthy volunteers, rather than attempting to use the ECG to identify an anatomical measure, as well as evaluating the prognostic performance of the ECG abnormality.

An abnormal vectorcardiographic QRS-T angle is not only an important sign of LVH<sup>11</sup>, but also an independent predictor of cardiovascular and all-cause mortality<sup>12–14</sup>. Clinical observations inspired the hypothesis that the vectorcardiographic QRS-T angle could provide diagnostic value beyond those of conventional ECG criteria for LVH. Therefore, the aims of this study were to a) propose a sex-specific upper limit of normal for the spatial

<sup>1</sup>Department of Clinical Physiology, Karolinska Institutet, and Karolinska University Hospital, Stockholm, Sweden. <sup>2</sup>Nicollier-Schlegel SARL, Trélex, Switzerland. <sup>3</sup>Department of Cardiology, Royal North Shore Hospital, Sydney, Australia. <sup>4</sup>Kolling Institute, Royal North Shore Hospital, University of Sydney, Kolling Building, Level 12, Room 612017, St Leonards, Sydney, NSW 2065, Australia. <sup>5</sup>International Laser Center CVTI, Bratislava, Slovak Republic. <sup>6</sup>Institute of Pathophysiology, Medical School, Comenius University, Bratislava, Slovak Republic. <sup>7</sup>Department of Medicine, University of Pittsburgh Medical Center, Pittsburgh, PA, USA. ✉email: martin.ugander@ki.se

peaks QRS-T angle derived from the resting 12-lead ECG, and b) investigate the diagnostic and prognostic performance of the QRS-T angle compared to conventional ECG criteria for LVH. We hypothesized that the QRS-T angle would provide diagnostic and prognostic value beyond that of conventional ECG criteria for LVH.

## Methods

**Participants and outcomes.** In this observational cohort study, patients were identified retrospectively from three prospectively acquired databases divided into four cohorts: (1) healthy volunteers used to define normality and a threshold for the QRS-T angle (Healthy-Derivation cohort), (2) healthy volunteers used to evaluate and compare the specificity of all studied measures (Healthy-Validation cohort), (3) clinical patients with at least moderate LVH by cardiac imaging, to evaluate the sensitivity of all studied measures (Imaging-LVH cohort), and (4) clinical patients referred for CMR imaging who also had follow-up data on hospitalization for heart failure or all-cause death, to evaluate the diagnostic and prognostic value of all studied measures (Clinical-Consecutive cohort). Mortality status was ascertained by medical record review and Social Security Death Index queries as previously described<sup>15</sup>. The study was approved by the local institutional review boards at University of Pittsburgh Medical Center, PA, USA, and NASA's Johnson Space Center, TX, USA and partner hospitals that fall under IRB exemptions for previously collected and de-identified data, respectively. All participants provided written informed consent, and all methods were carried out in accordance with relevant guidelines and regulations. Data can be made available upon reasonable request.

**Healthy volunteer cohorts.** A database with digital ECG recordings from healthy volunteers was divided into two parts where two thirds were used for Healthy-Derivation, and one third for Healthy-Validation. The Healthy-Derivation and Healthy-Validation cohorts were included from three different sites in the USA, as previously described in detail<sup>16</sup>. Briefly, all healthy volunteers were low risk and asymptomatic, without evidence of cardiovascular or other systemic disease based on a physical examination and negative history, and with a clinically normal conventional ECG. If LVH or hypertrophic cardiomyopathy was suspected based on clinical assessment of the ECG, an echocardiogram was performed to rule out the given suspected pathology(s), and the subject was not included in any of the Healthy cohorts. Asymptomatic volunteers who received treatment for diabetes, hypertension, or active smokers were excluded.

**Imaging-LVH cohort.** The Imaging-LVH cohort was included from seven different sites in the USA, Sweden, and Venezuela, as previously described in detail<sup>16</sup>. Briefly, inclusion criteria for the Imaging-LVH cohort was an ECG acquired within 30 days of the cardiac imaging examination. The Imaging-LVH cohort was limited to at least moderate LVH by imaging for the purposes of evaluating the sensitivity of the ECG criteria in a population with definite LVH. Exclusion criteria were a non-sinus or paced rhythm, left or right bundle branch block, pre-excitation, an incomplete ECG recording, and imaging findings of a predominant cardiac pathology other than LVH, such as myocardial infarction or extensive non-ischemic scarring by CMR, or at least moderate valvular disease by echocardiography.

**Clinical-Consecutive cohort.** The Clinical-Consecutive cohort included consecutive patients referred clinically for CMR at University of Pittsburgh Medical Center, PA, USA, between 2008 and 2017, and with follow-up until April 2018. Inclusion criteria for the Clinical-consecutive cohort were an ECG with sinus rhythm and a QRS duration < 120 ms, and an ECG acquired within 30 days of the CMR examination. Exclusion criteria were ECG confounders such as atrial fibrillation or flutter, abundant premature ventricular contractions (bigeminy/trigeminy), paced rhythm, hypertrophic cardiomyopathy, congenital heart disease, Takotsubo cardiomyopathy, amyloidosis, siderosis, Fabry's disease, and poor CMR image quality.

**ECG acquisition and analysis.** ECG data for the healthy volunteers and Imaging-LVH cohorts included resting 12-lead ECG acquired at 1000 Hz sampling rate, with an acquisition duration of at least 10 s. ECG data for the Clinical-Consecutive cohort was collected from the local clinical digital ECG database (MUSE® Cardiology Information System, Version 8.0 SP2, GE Healthcare, Chicago, IL, USA) and exported into anonymized .xml files with coded subject identification. ECG data for the Clinical-Consecutive cohort included resting 12-lead ECG acquired at sampling rates of 250 or 500 Hz, with an acquisition duration of 10 s. The following conventional ECG variables were automatically analyzed using in-house developed software<sup>16</sup> according to established published criteria: Sokolow-Lyon index, defined as the sum of the S wave in lead V1 ( $S_{V1}$ ) plus the larger of the  $R_{V5}$  or  $R_{V6}$ , where LVH was defined as  $>3.5$  mV<sup>17</sup>; Cornell voltage, defined as  $S_{V3}$  plus  $R_{aVL}$ , where LVH was defined as  $>2.0$  mV for females and  $>2.8$  mV for males<sup>18</sup>; Cornell product, defined as the QRS duration times the Cornell voltage, where LVH was defined as  $\geq 244$  mV·ms<sup>19</sup>; and the QRS duration, based on the automatic measurement output from the given ECG machine vendor, where increased QRS duration was defined as  $\geq 100$  ms<sup>20</sup>. The vectorcardiogram was derived from the resting 12-lead ECG using the previously validated Kors' regression method<sup>21</sup>, and the derived spatial peaks QRS-T angle was defined as the angular difference, in three-dimensional space, between the maximum magnitude of the vectors of the QRS and T loops, respectively<sup>22</sup>. See Fig. 1 for a schematic illustration of the spatial peaks QRS-T angle, and Fig. 2 for ECGs from two representative cases from the study.

**Echocardiographic and cardiovascular magnetic resonance imaging analysis.** In the Imaging-LVH cohort, LVH was defined as being at least moderate according to the guidelines of the American Society of Echocardiography<sup>23</sup>. In the Clinical-Consecutive cohort, LVH was defined as either a left ventricular mass index

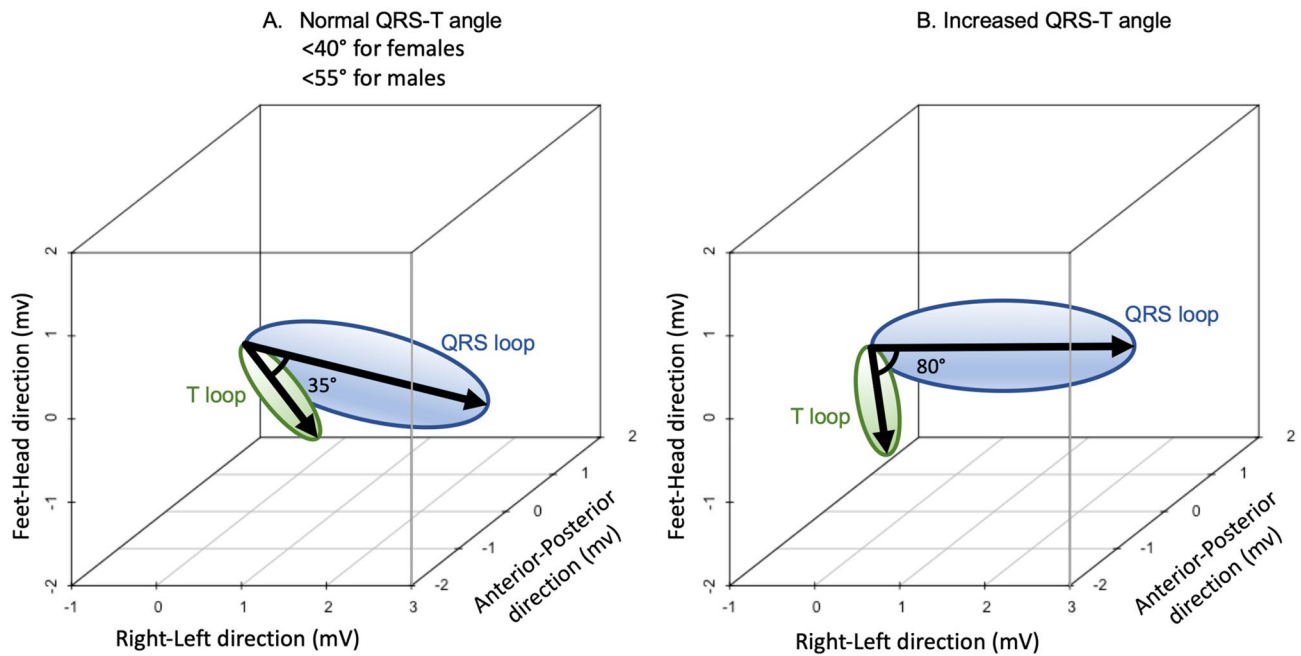


**Figure 1.** Schematic illustration of the QRS-T angle, a vectorcardiographic measure derived from a digital resting 12-lead ECG. The vectorcardiogram represents the electrical activity in millivolts (mV) in three dimensions along the left–right, feet–head and anterior–posterior axes. The QRS loop (blue) and T loop (green) represent the direction and peak magnitude of depolarization and repolarization, respectively, of the left ventricle. The thick arrows show the largest magnitudes of the respective loops. The angle in three-dimensional space between the largest magnitude of the QRS loop and T loop is referred to as the spatial peaks QRS-T angle. (A) Schematic example of a normal QRS-T angle of  $35^\circ$  in a healthy volunteer. (B) Schematic example of an increased QRS-T angle of  $80^\circ$ .

(LVMI) or left ventricular end diastolic volume index (LVEDVI) greater than the 95% upper limit of normal for age- and sex-matched healthy volunteers with no history of cardiac disease or known risk factors according to published normal values<sup>24</sup>. The Clinical-Consecutive cohort underwent CMR to define measures known to associate with prognosis. These measures included left ventricular global longitudinal strain (GLS), which is a marker for impaired left ventricular function, left ventricular ejection fraction (LVEF), myocardial extracellular volume fraction (ECV), LVMI, LVEDVI, infarct size, and non-ischemic scar size. These measures were acquired and quantified according to clinical standards as previously described in detail<sup>25</sup>.

**Statistical analysis.** Statistical analysis was performed in R version 3.4.3 (R Foundation for Statistical Computing, Vienna, Austria). The sex-specific cut-off for an increased derived spatial peaks QRS-T angle was defined as the upper limit of the 95% confidence interval of normal in the Healthy-Derivation cohort. The sensitivity to detect LVH by the QRS-T angle was evaluated in the Imaging-LVH and Clinical-Consecutive cohorts, respectively. The specificity to detect LVH by the QRS-T angle was evaluated in the Healthy-Validation and Clinical-Consecutive cohorts, respectively. The area under the receiver operating characteristic curve (AUC) was evaluated in the combined Healthy-Validation and Imaging-LVH cohorts to include participants and patients with and without LVH, and Clinical-Consecutive cohort, respectively, with respect to the QRS-T angle and the conventional ECG criteria for LVH, and compared using DeLong's test. Linear correlations between the QRS-T angle and conventional criteria in the respective cohorts were evaluated using Pearson's correlation coefficient, and expressed as its square ( $R^2$ ).

Using univariable Cox regression and Kaplan–Meier analysis, the QRS-T angle and conventional ECG measures for LVH were also compared in their ability to predict the combined, and individual, outcome of survival free from hospitalization for heart failure or all-cause death, ranking each according to the Wald chi-square value. Multivariable Cox regression was performed using measures that were not mathematically related to each other, and also significantly associated with outcomes in univariable Cox regression. Hazard ratios were analyzed as binary variables with cut-offs for LVH, as described above, as these cut-offs are used clinically. To investigate whether the QRS-T angle and conventional criteria correctly classified LVH in the same patients, the percentage of agreement, and Cohen's kappa statistic were calculated. To further investigate the incremental prognostic value for the QRS-T angle, net reclassification index (NRI) was calculated in the Clinical-Consecutive cohort at one year of follow-up. NRI can be used to show the correctness of reclassification of subjects based on a new model, and calculated as<sup>26</sup>:  $NRI = (\text{number of correctly reclassified events} - \text{number of incorrectly reclassified events}) + (\text{number of correctly reclassified nonevents} - \text{number of incorrectly reclassified nonevents})$ . The adjusted R-square ( $R^2$ ) in multivariable linear regression was used to evaluate the combined relative contributions of CMR measures to the QRS-T angle. The Kolmogorov–Smirnov test was used to test if data was normally

## Conventional 12-lead ECG

## Corresponding vectorcardiogram showing the spatial QRS-T angle

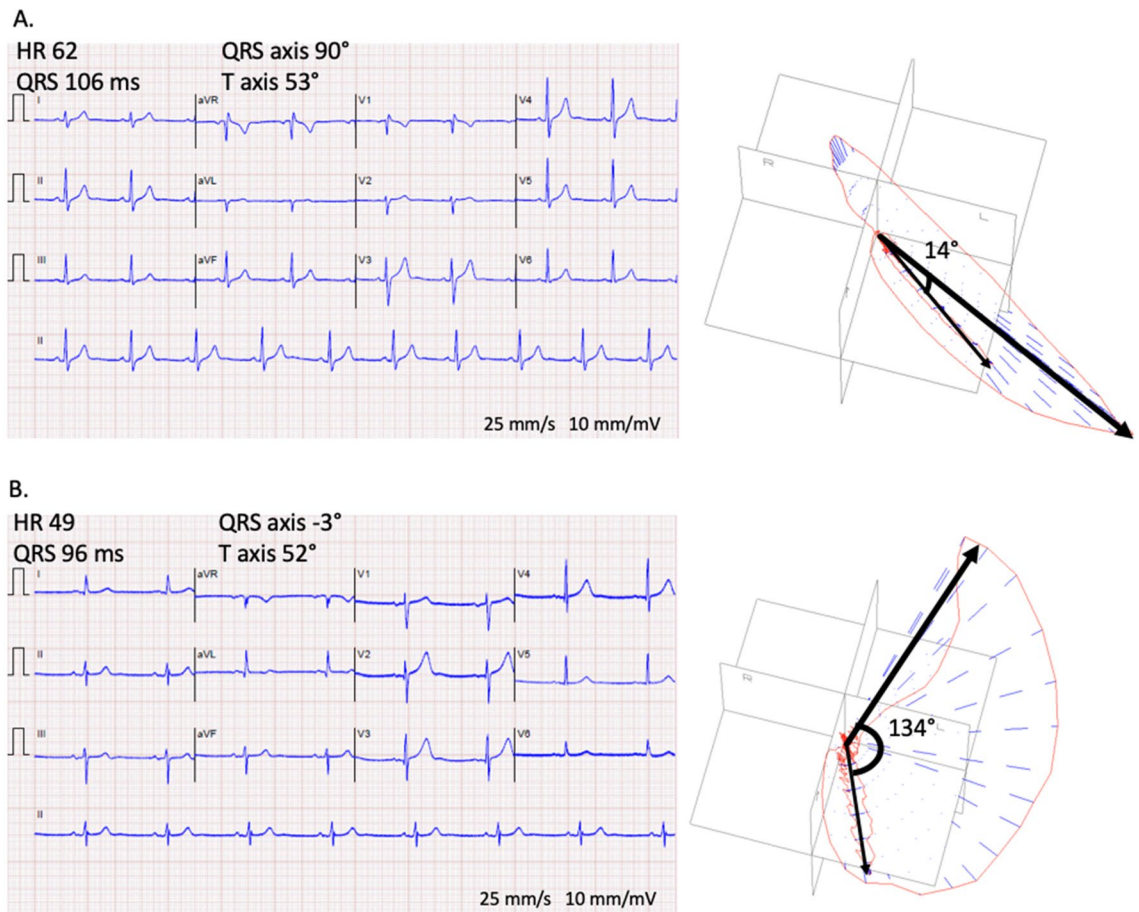


**Figure 2.** Two representative examples of different QRS-T angles from the study. (A) A normal conventional 12-lead ECG in a healthy male in their 50s, with a corresponding derived vectorcardiographic spatial peaks QRS-T angle of 14° (normal). (B) A normal conventional 12-lead ECG in a male in their 80s with imaging-proven LVH, with a corresponding derived spatial peaks QRS-T angle of 134° (abnormal). HR denotes heart rate. Note, the QRS axis and T axis noted in the figure are from the frontal plane, whereas the spatial peaks QRS-T angle is calculated in three-dimensional space from the derived vectorcardiogram.

distributed, and differences between subgroups' baseline data was tested using the Mann–Whitney U test or chi-square test, as appropriate, and described using the median [interquartile interval], or percentage, respectively. A  $p$ -value < 0.05 was considered statistically significant.

## Results

**Baseline characteristics.** A total of 2390 patients and healthy volunteers with QRS duration < 120 ms and an ECG without rhythm confounders were included in the four cohorts: Healthy-Derivation ( $n = 921$ , age 34 [27–48] years, full range 20–85 years, 39% female), Healthy-Validation ( $n = 461$ , age 35 [27–48] years, 39% female), Imaging-LVH ( $n = 225$ , age 63 [53–75] years, 60% female), and Clinical-Consecutive ( $n = 783$ , age 55 [43–64] years, 44% female). A total of 30 females and 28 males in the Healthy-Derivation cohort were  $\geq 60$  years old. The Healthy-Derivation and Healthy-Validation cohorts did not differ with respect to age and sex distribution. The baseline characteristics of the Clinical-Consecutive cohort are presented in Table 1. In the Clinical-Consecutive cohort, 155 patients experienced events over a follow-up period of 5.7 [4.4–6.6] years: 113 (14.4%) deaths, 68 (8.7%) hospitalizations for heart failure, and 26 (3.3%) with both. Compared to patients with a normal QRS-T angle, patients with an increased QRS-T angle had more CMR abnormalities, including LVH, and cardiovascular co-morbidities at baseline, reflecting a greater severity or burden of cardiovascular disease.

**Normal values for the QRS-T angle.** The Healthy-Derivation cohort was used to define the upper limit of the sex-specific 95% confidence interval of normal for the derived QRS-T angle. In this cohort of healthy volunteers, the upper limit of normal for the QRS-T angle differed with regards to sex but not age (results not shown). Consequently, sex-specific normal values were presented for the whole cohort regardless of age. The

Characteristic	All	Normal QRS-T angle	Increased QRS-T angle	p value
Number, n (%)	783 (100)	377 (48)	406 (52)	n/a
Age, y	55 (43 to 64)	53 (38 to 62)	57 (46 to 65)	<0.001
Female sex, %	342 (44)	149 (40)	193 (48)	0.02
LVH	227 (29)	59 (18)	168 (41)	<0.001
ECV, %	27.6 (25.3 to 30.3)	26.8 (24.8 to 29.1)	28.5 (25.7 to 31.1)	<0.001
EDVI, mL/m <sup>2</sup>	78.3 (66.1 to 97.3)	74.5 (63.7 to 89.3)	84.5 (67.6 to 111.2)	<0.001
GLS, %	-16.2 (-18.8 to -12.3)	-17.6 (-19.5 to -15.3)	-13.9 (-17.3 to -9.8)	<0.001
LVEF, %	58.5 (47.0 to 65.0)	61.0 (55.3 to 66.0)	55.0 (34.3 to 63.0)	<0.001
LVMI, g/m <sup>2</sup>	55.3 (44.9 to 67.1)	51.7 (43.6 to 61.4)	59.4 (46.8 to 73.8)	<0.001
BMI, kg/m <sup>2</sup>	28.6 (24.4 to 33.9)	28.3 (24.4 to 33.5)	29.0 (24.4 to 34.0)	0.41
BSA, m <sup>2</sup>	2.0 (1.8 to 2.2)	2.0 (1.8 to 2.2)	2.0 (1.8 to 2.2)	0.28
Infarct, n (%)	165 (21)	43 (11)	122 (30)	<0.001
Infarct size*, %	14.7 (5.9 to 22.3)	8.8 (4.4 to 17.5)	15.8 (7.7 to 24.1)	<0.001
Non-ischemic scar, n (%)	137 (17)	50 (13)	87 (21)	0.003
Non-ischemic scar size*, %	2.9 (1.5 to 5.7)	2.6 (0.7 to 6.1)	2.9 (1.5 to 5.1)	0.50
<b>Conventional ECG-LVH criteria</b>				
Sokolow-Lyon index, mV	1.8 (1.4 to 2.3)	1.7 (1.4 to 2.2)	1.9 (1.4 to 2.1)	0.39
Cornell voltage, mV	1.4 (1.0 to 1.8)	1.2 (0.95 to 1.6)	1.6 (1.2 to 2.1)	<0.001
Cornell product, mV*ms	132 (94 to 176)	114 (82 to 150)	152 (110 to 206)	<0.001
QRS duration, ms	90 (84 to 98)	88 (82 to 96)	92 (84 to 100)	0.03
<b>Comorbidity, n, (%)</b>				
Hypertension	398 (51)	158 (42)	240 (52)	<0.001
Diabetes mellitus	171 (22)	57 (15)	114 (25)	<0.001
<b>Smoking status, n, (%)</b>				
Current smoker	129 (16)	47 (12)	82 (18)	0.004
Ex-smoker	246 (31)	112 (30)	134 (29)	0.32
<b>Medication, n, (%)</b>				
ACEi/ARB	315 (40)	114 (30)	201 (44)	<0.001
Aspirin or other antiplatelets	397 (51)	157 (42)	240 (52)	<0.001
Beta-blockers	387 (49)	143 (38)	244 (53)	<0.001
Digoxin	23 (3)	4 (1)	19 (5)	0.01
Insulin	121 (15)	40 (11)	81 (17)	<0.001
Loop diuretics	164 (21)	45 (12)	119 (26)	<0.001
Oral hypoglycemics	54 (7)	12 (3)	42 (9)	<0.001
Statins	315 (40)	124 (33)	191 (42)	<0.001
<b>General indication for CMR: known or suspected disease, n (%)</b>				
Arrhythmia or syncope	147 (19)	59 (16)	88 (22)	0.03
Coronary artery disease/vasodilator stress test	365 (47)	230 (61)	135 (33)	<0.001
Dyspnea	56 (7)	38 (10)	18 (4)	0.002
Non-ischemic cardiomyopathy	181 (23)	114 (38)	67 (17)	<0.001
Pre-operation evaluation	37 (5)	21 (6)	16 (4)	0.28
Valvular disease	48 (6)	24 (6)	24 (6)	0.79

**Table 1.** Baseline characteristics for the Clinical-Consecutive cohort. Continuous data are given as median (interquartile interval), or number (%), and compared between the Normal QRS-T angle group and Increased QRS-T angle groups using Mann–Whitney U test or Chi-square, respectively. ACEi Angiotensin-converting enzyme inhibitors, ARB Angiotensin II receptor blocker, BMI Body mass index, BSA Body surface area, CMR Cardiovascular magnetic resonance imaging, ECV Extracellular volume fraction, LVEDVI Left ventricular end-diastolic volume index, GLS Global longitudinal strain, LVEF Left ventricular ejection fraction, LVMI Left ventricular mass index. \*Denotes that the descriptive data are presented only for those patients with infarct or non-ischemic scar, respectively.

mean values  $\pm$  1.96 SD for the QRS-T angle were  $19.7 \pm 19.9^\circ$  for females and  $26.6 \pm 28.3^\circ$  for males. This yielded sex-specific thresholds for the QRS-T angle of  $\geq 40^\circ$  for females, and  $\geq 55^\circ$  for males.

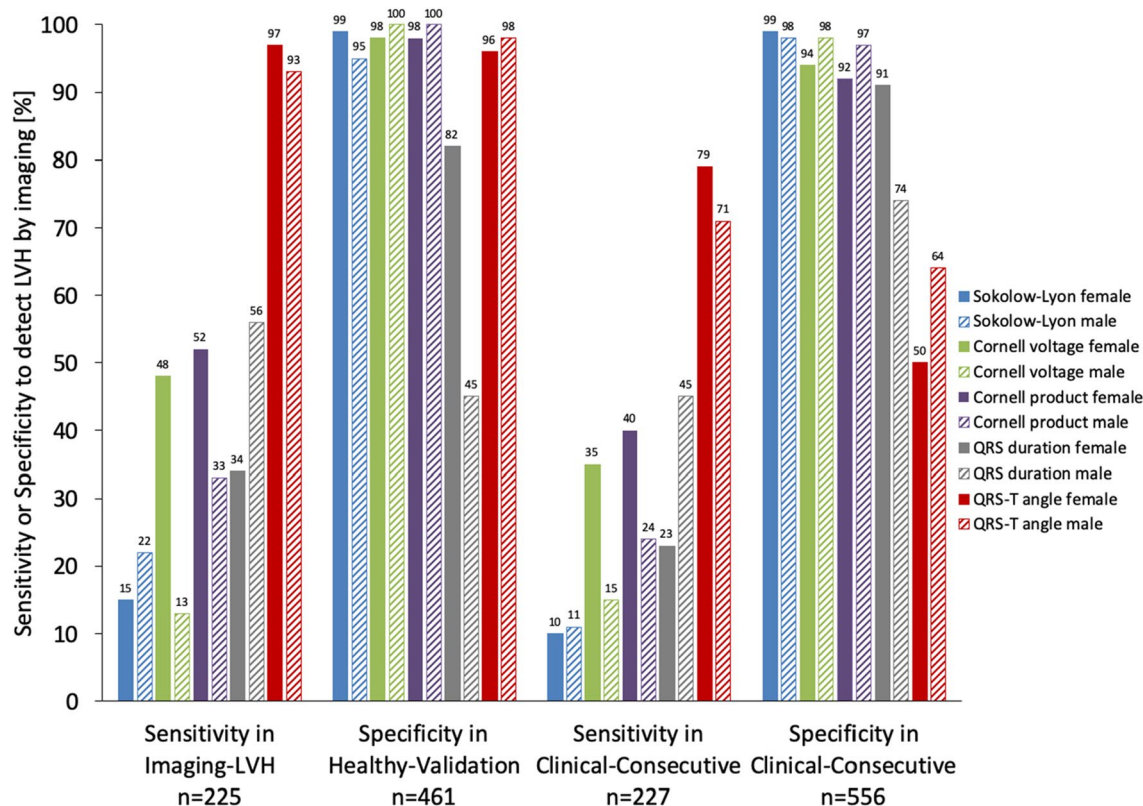


**Figure 3.** Sex-specific sensitivity or specificity for detecting anatomically defined left ventricular hypertrophy (LVH) in the respective cohorts. In both the Imaging-LVH and Clinical-Consecutive cohorts, an increased QRS-T angle had a higher sensitivity for LVH than all other ECG measures ( $p < 0.05$  for all). Among females in the Healthy-Validation cohort, the specificity of the QRS-T angle for LVH was higher than that of QRS duration ( $p < 0.001$ ), lower than Cornell product ( $p < 0.05$ ), and did not differ significantly from that of the other measures ( $p > 0.05$  for all). Among males in the Healthy-Validation cohort, the specificity of the QRS-T angle for LVH was higher than that of QRS duration ( $p < 0.001$ ), lower than Cornell voltage and Cornell voltage product ( $p < 0.05$  for both), and did not differ significantly from Sokolow-Lyon index ( $p = 0.12$ ). In the Clinical-Consecutive cohort, the QRS-T angle had a lower specificity than the other ECG measures ( $p < 0.05$  for all) despite its excellent specificity in the Healthy-Validation cohort, suggesting possible electrical identification of subclinical disease in patients who do not yet fulfill imaging criteria for LVH.

**The QRS-T angle in imaging-verified LVH.** The specificity of the QRS-T angle in the Healthy-Validation cohort was 172/180 (96%) in females and 274/281 (98%) in males. In the Imaging-LVH cohort, the sensitivity of the QRS-T angle for detecting LVH was higher than that of conventional ECG criteria (93–97% vs 13–56%,  $p < 0.001$  for all, see Fig. 3), illustrating that an increased QRS-T angle is present in nearly all LVH of moderate or greater severity, and to a far greater extent than positive conventional ECG criteria for LVH. In the Clinical-Consecutive cohort, the sensitivity of the QRS-T angle for detecting any LVH defined as a LVMI or a LVEDVI above the upper limit of normal by CMR was 54/77 (79%) in females and 105/150 (71%) in males, again superior to that of the conventional ECG criteria ( $p < 0.001$  for all). In the Clinical-Consecutive cohort, the specificity of the QRS-T angle for LVH was 133/265 (50%) in females and 185/291 (64%) in males, and was lower compared to that of the conventional criteria ( $p < 0.01$  for all). Of the patients in the Clinical-Consecutive cohort who did not have any LVH, 238/556 (43%) had an increased QRS-T angle.

In the Clinical-consecutive cohort, a total of 19 patients (8%) with LVH were detected by both the Sokolow-Lyon index and the QRS-T angle, 47 patients (21%) by both Cornell voltage and the QRS-T angle, 46 patients (20%) by both Cornell product and the QRS-T angle, and 64 patients (28%) by both the QRS duration and the QRS-T angle, respectively. The QRS-T angle had a 50%, 57%, 55% and 51% agreement in correctly classified cases and non-cases with the Sokolow-Lyon Index, Cornell voltage, Cornell Product, and QRS duration, respectively, yielding a Cohen's kappa ( $p$  value) of  $-0.13$  ( $< 0.001$ ),  $0.17$  ( $< 0.001$ ),  $0.13$  ( $0.001$ ), and  $0.04$  ( $0.20$ ), respectively. In the combined Healthy-Validation and Imaging-LVH cohort, the QRS-T angle had a higher AUC (AUC 0.99) than all conventional parameters (AUC 0.53–0.91) for detecting LVH ( $p < 0.001$  for all), see Fig. 4. In the Clinical-Consecutive cohort, the AUC for the QRS-T angle (AUC 0.72) did not differ significantly from Cornell voltage (AUC 0.69), Cornell voltage product (AUC 0.71), nor QRS duration (AUC 0.65) ( $p > 0.19$  for all), see Fig. 4.

In the Clinical-Consecutive cohort, the QRS-T angle was correlated to the Cornell voltage and Cornell product, respectively ( $R^2 = 0.20$  and  $p < 0.001$  for both). In the other cohorts there was a weaker correlation between the QRS-T angle and the conventional parameters ( $R^2$  ranging from  $< 0.01$  to  $0.11$ ).

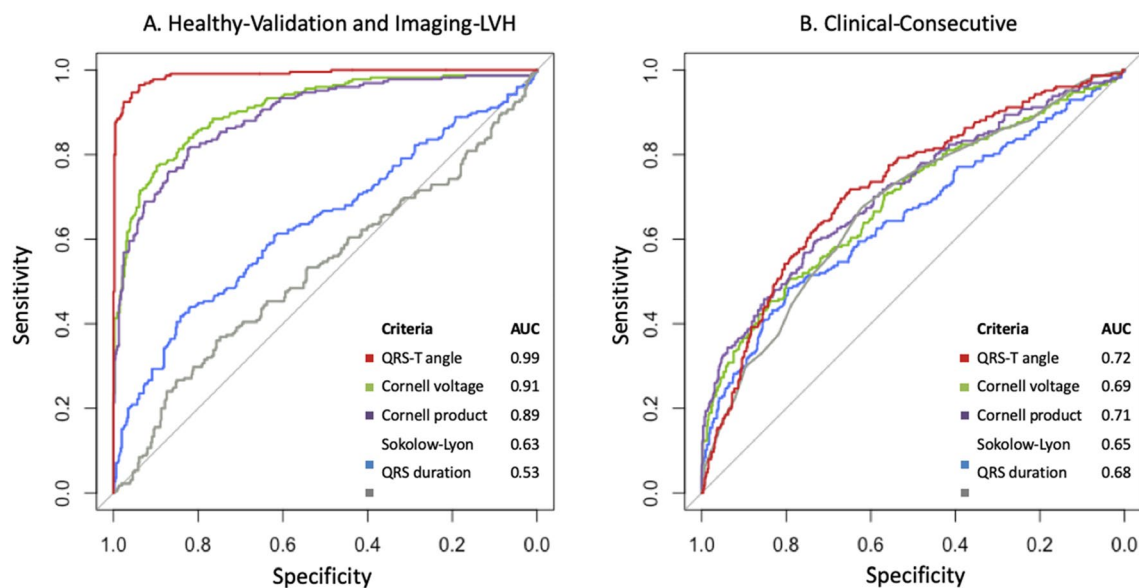


**Figure 4.** Area under the curve (AUC) for the evaluated criteria for detecting anatomically defined left ventricular hypertrophy. **(A)** AUC for the criteria in the combined Healthy-Validation and Imaging-LVH cohorts. **(B)** AUC for the criteria in the Clinical-Consecutive cohort.

Covariates	Univariable Cox regression model			Multivariable Cox regression model		
	$\chi^2$	Hazard ratio (95% CI)	<i>p</i> value	$\chi^2$	Hazard ratio (95% CI)	<i>p</i> value
QRS-T angle	22	2.27 (1.62–3.20)	<0.001	20	2.22 (1.56–3.16)	<0.001
Cornell product	24	2.53 (1.74–3.67)	<0.001	–	–	–
QRS duration	18	2.02 (1.45–2.80)	<0.001	16	1.99 (1.42–2.77)	<0.001
Cornell voltage	7	1.81 (1.15–2.84)	0.006	0.2	1.12 (0.70–1.81)	0.63
Sokolow-Lyon	1	1.45 (0.71–2.96)	0.30	–	–	–

**Table 2.** Uni- and multivariable Cox regression analysis for the QRS-T angle, QRS duration, Cornell voltage product, Cornell voltage, and Sokolow-Lyon index in the Clinical-Consecutive cohort for predicting the composite outcome of hospitalization for heart failure and all-cause mortality. Covariates were analyzed as binary variables with cut-offs for left ventricular hypertrophy. See text for details on cut-offs. Cornell product was not included in multivariable analysis due to being mathematically related to QRS duration and Cornell voltage.

**The QRS-T angle in LVH and outcomes.** Per Table 2, univariable Cox analysis showed that the QRS-T angle and Cornell product both had a high univariable association with outcomes (chi-square 22 and 24, respectively,  $p < 0.001$  for both). Cornell voltage product had a hazard ratio and 95% confidence interval (95% CI) of 2.53 (1.74–3.67), and the QRS-T angle had a hazard ratio of 2.27 (1.62–3.20). Furthermore, an increased QRS-T angle was associated with both components of the combined outcome hospitalization for heart failure and all-cause mortality (chi-square 21 and 10, respectively,  $p < 0.001$  and  $p < 0.01$ , respectively) with a hazard ratio of 3.94 (2.19–7.10), and 1.86 (1.26–2.73), respectively. In multivariable Cox analysis, the Sokolow-Lyon index was excluded due to the absence of an association with outcomes in univariable analysis, and Cornell product was excluded due to both being mathematically related to both QRS duration and Cornell voltage. Multivariable Cox regression showed an association with outcomes for both the QRS-T angle (hazard ratio 1.95 (1.36–2.80),  $p < 0.001$ ) and QRS duration (hazard ratio 1.99 (1.42–2.77),  $p < 0.001$ ), but not for Cornell voltage (hazard ratio 1.12 (0.70–1.81),  $p = 0.63$ ). When comparing the QRS-T angle to co-morbidities, multivariable Cox regression showed an association with outcomes for the QRS-T angle criterion (hazard ratio 1.68 (1.18–2.38),  $p = 0.004$ ), hypertension (hazard ratio 1.96 (1.34–2.87),  $p < 0.001$ ), and diabetes mellitus (hazard ratio 2.63 (1.88–3.68),  $p = 0.004$ ), but not for smoking status. Figure 5 shows Kaplan-Meier analysis illustrating the poorer event-free survival for patients with an increased QRS-T angle compared to those with a normal QRS-T angle ( $p < 0.001$ ). The NRI analysis showed an incremental prognostic value of the QRS-T angle beyond the Cornell product with a NRI of 0.40 (95% CI 0.02–0.66).

**Relationship between the QRS-T angle and CMR measures.** The QRS-T angle correlated with GLS, ECV, LVEDVI, LVMI, infarct size, and non-ischemic scar size ( $R^2 = 0.01$ –0.25,  $p < 0.05$  for all). In multivariable

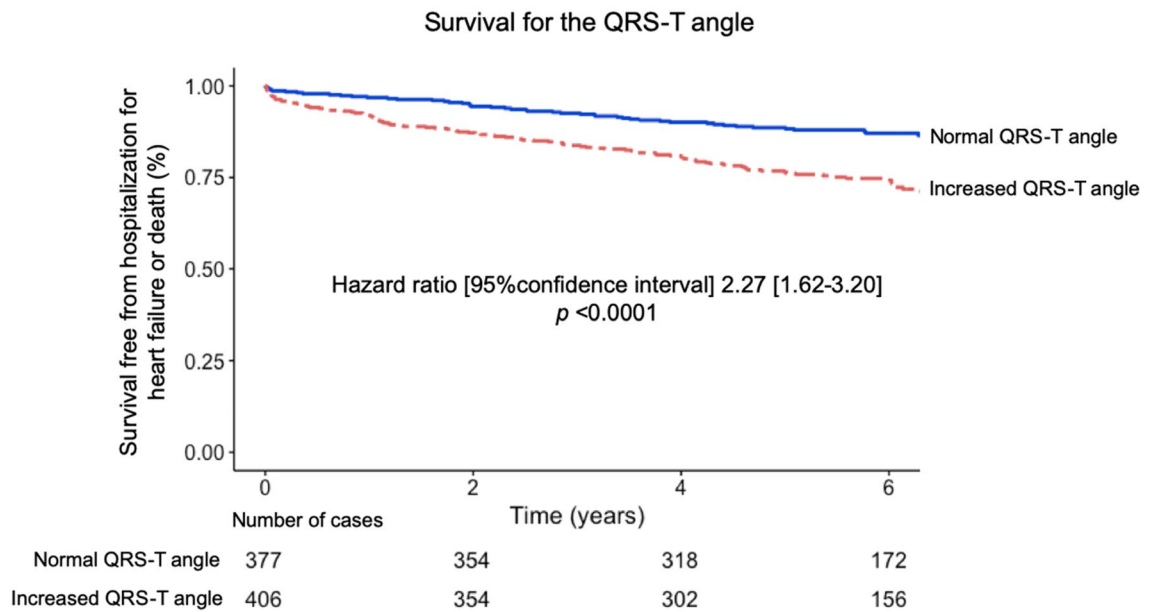


**Figure 5.** Outcomes for patients in the Clinical-Consecutive cohort according to the presence of a normal or increased derived spatial peaks QRS-T angle, respectively, defined as  $\geq 40^\circ$  for females and  $\geq 55^\circ$  for males. An increased QRS-T angle was associated with worse outcomes in the form of survival free from heart failure hospitalization or all-cause death with events in 155 patients over a follow-up period of 5.7 [4.4–6.6] years.

able analysis, GLS, ECV, LVMI, and infarct size remained associated with the QRS-T angle (adjusted  $R^2 = 0.28$ ,  $p < 0.001$ ).

## Discussion

The major finding of this study was that, compared to existing ECG criteria for LVH, the proposed QRS-T angle criteria substantially improved sensitivity and preserved excellent specificity for identifying moderate or greater anatomical LVH in the Imaging-LVH cohort with at least moderate LVH by imaging. Furthermore, the QRS-T angle also provided important information for risk stratification and outcomes in a population with underlying cardiovascular comorbidities, representative of patients with suspected heart disease, that was independent of that from the Cornell voltage and QRS duration, respectively, in multivariable analysis. The current study also found that an increased QRS-T angle is common even among patients referred for clinical CMR who had normal LVMI. Furthermore, abnormal QRS-T angle was exceedingly rare in the Healthy-Validation sub-cohort, which could be expected given that both the Healthy-Derivation and Healthy-Validation groups were randomly selected from the same larger cohort of healthy volunteers. This illustrates that the QRS-T angle identifies an electrical remodeling process often missed by anatomical imaging. This finding is in agreement with the previous finding that anatomical LVH and conventional ECG criteria for LVH possess independent prognostic information<sup>9</sup>.

**The spatial peaks QRS-T angle.** The spatial peaks QRS-T angle is an established vectorcardiographic measure that can be derived from a standard digital 12-lead ECG. It is defined as the angle in three-dimensional space between the peak magnitude of the vectors for the QRS and T loops, respectively. Similarly to the concordance or discordance between the QRS complex and T waves in a given lead of the conventional ECG, the QRS-T angle reflects the dispersion between the directions of left ventricular depolarization and repolarization<sup>27</sup>. In a healthy heart, the angle between the QRS and T loops is small, whereas the angle has been shown to increase as a result of myocardial disease processes (Figs. 1, 2)<sup>13</sup>. On the conventional ECG, repolarization changes such as ST depression and T wave inversion, sometimes referred to as strain, are also known markers of LVH with reported sensitivities and specificities of up to 52% and 95%, respectively<sup>28</sup>. Due to a combination of structural, bioelectrical and biochemical changes in LVH<sup>29</sup>, the electrical propagation is interrupted, contributing to changes in depolarization and repolarization that usually increase the QRS-T angle. Regardless, the spatial peaks QRS-T angle was only weakly correlated to conventional ECG criteria, and more sensitive at detecting LVH compared to conventional ECG criteria that rely upon increased QRS amplitudes or durations. Moreover, by quantifying discordance between depolarization and repolarization, the spatial peaks QRS-T angle also introduces prognostic information independent of QRS amplitude and duration as quantified by Cornell product. There is no previously established QRS-T angle cut-off, and previous studies have used different cut-off values<sup>30</sup>. Such cut-offs have been based on a general elderly population<sup>31</sup>, postmenopausal women<sup>32</sup>, and patients undergoing clinically indicated cardiac exams<sup>33,34</sup>. The current study based the sex-specific cut-offs on a large group of healthy individuals with a wide age range of 20–85 years.

The QRS-T angle has historically been measured by vectorcardiography using acquisition with dedicated lead placement. Vectorcardiography was largely abandoned as a widely used clinical tool in the latter half of the



twentieth century due to a combination of technical, interpretation-related, and acquisition standardization-related complexities. However, in today's healthcare environment, the conventional 12-lead ECG is typically digitally recorded and stored. Consequently, validation of techniques that accurately derive the vectorcardiogram from the digital 12-lead ECG<sup>21</sup> have now made it trivial to automatically and accurately calculate, visualize, and access vectorcardiographic measures including the QRS-T angle.

**Anatomy versus electrocardiography.** In the current study, abnormal QRS-T angle was both effectively absent in an independent cohort of healthy volunteers, but present in nearly all patients with imaging-proven, at least moderate, LVH without other predominant cardiac morbidities. The QRS-T angle had a markedly different diagnostic accuracy in the Imaging-LVH and Clinical-Consecutive cohorts, likely due to the presence of intermediate disease in the Clinical-Consecutive cohort, whereas the Imaging-LVH cohort was only based on the presence of moderate or severe LVH. Hence, the presence of intermediate disease, including coronary artery disease without LVH<sup>16</sup>, could also increase spatial QRS-T angle values and thus have decreased the diagnostic discriminatory ability in the Clinical-Consecutive cohort. Furthermore, 47% of the Clinical-Consecutive patients underwent a clinical CMR scan due to known or suspected coronary artery disease, potentially reflecting a higher likelihood for presence of disease potentially affecting electrical propagation beyond cardiomyocyte hypertrophy as such. The intermediate diagnostic performance of the QRS-T angle compared to anatomical criteria in the Clinical-Consecutive cohort further underscores the inappropriateness of judging the utility of electrocardiographic criteria using an anatomical arbiter. Due to the known lack of association between electrocardiographic changes and anatomical or structural changes<sup>29</sup>, outcomes may be a more appropriate arbiter of diagnostic utility. In fact, the QRS-T angle was associated with prognosis, even beyond that of the conventional criteria with the best performance in both multivariable analysis and NRI analysis. The QRS-T angle had approximately a 50% agreement with the conventional parameters, and a Cohen's kappa close to 0, indicating that they did not identify the same patients.

**Associations between the QRS-T angle and either CMR or co-morbidities.** Compared to patients in the Clinical-Consecutive cohort who had a normal QRS-T angle, those with an increased angle had CMR or clinical demographic characteristics that are associated with a greater severity or burden of cardiovascular disease, with the exception of body mass index, body surface area, and non-ischemic scar size. Despite this, CMR parameters known to convey powerful prognostic information could together only explain approximately one quarter of the QRS-T angle (adjusted  $R^2 = 0.28$ ). This illustrates the complementary information present in the ECG compared to structural and functional measures assessable by imaging. Other groups have also reported a superiority of the QRS-T angle compared to conventional ECG criteria for LVH<sup>11</sup>, and that the QRS-T angle is increased in patients with co-morbidities such as hypertension<sup>35</sup> and diabetes<sup>36</sup>. However, the current study is unique in that it studied robust sample sizes to both propose sex-specific upper limits of normal for the QRS-T angle, and undertake a comprehensive and definitive approach to evaluation of diagnostic and prognostic performance. Besides the QRS-T angle, the QRS duration was an independent predictor of outcomes, even though patients with complete bundle branch blocks were excluded, while no voltage-related criteria remained associated with outcomes.

**Clinical perspectives.** The present study shows a markedly improved diagnostic and prognostic performance of the newly proposed QRS-T angle criterion compared to currently used ECG criteria, suggesting that it provides diagnostic and prognostic information beyond the conventional ECG measures of LVH. The results highlight the difference between the electrocardiographic and anatomical manifestations of disease, and underscore the necessity to define ECG abnormalities as a deviation from ECG normal values in healthy volunteers rather than as defined by anatomical findings. The Journal of Electrocardiology LVH Working Group<sup>10</sup> has proposed that electrical changes associated with LVH may be better defined as LVER as opposed to LVH by ECG. Furthermore, replacing the term LVH with LVER in the evaluation of the ECG has the pedagogical advantage of clarifying the distinction between anatomical and electrical changes associated with remodeling. The current study suggests that an increased QRS-T angle could be used to define LVER, and that the concept of LVER should replace LVH whenever electrical changes are being addressed.

Assessment of the spatial peaks QRS-T angle requires a digitally acquired resting 12-lead ECG and software-based determination. Such solutions may not be available in all clinical settings, but the results of the current study suggest that such implementations may be worth considering. If necessary, the spatial peaks QRS-T angle can also be manually estimated from paper-based 12-lead ECGs using established techniques<sup>37</sup>, albeit likely with some compromise in precision and accuracy. Importantly, the presentation of this measure can be easily implemented in a wholly automated fashion into the software of digital ECG machines, and displayed together with conventional parameters and criteria at the time of clinical interpretation.

**Study limitations.** Our results are not applicable to patients with QRS duration > 120 ms, in whom the QRS-T angle is usually increased, especially in left bundle branch block due to the block itself. Similarly, our results are not applicable to patients with atrial fibrillation or other pathological arrhythmias, whom we excluded due to the known poorer prognosis associated with such arrhythmias<sup>38</sup>. The prognostic implications are based on a limited time period with a median of 5.7 years, and no interventions were performed as part of the study. Studies with interventions and with longer follow up times would be justified. The mean age in the healthy cohorts was younger than those in the Imaging-LVH and Clinical-Consecutive cohorts. As isolated LVH on the ECG is common in younger individuals, the specificity in the healthy cohort would be expected to be lower. Still, the specificity of the QRS-T angle remained high in the Healthy-Validation cohort. Notably, the Healthy-

Derivation cohort included an adequate number of subjects over the age of 60 years, and no age differences in the healthy normal range of the QRS-T angle were noted. However, the QRS-T angle could potentially increase with other characteristics that were not evaluated in the current study, and this is a limitation. Furthermore, the 95% upper limit of normal was used to define cut-offs for the QRS-T angle in a large cohort of healthy volunteers, excluding extreme outliers. We did not attempt to distinguish between eccentric hypertrophy from concentric hypertrophy. The QRS-T angle was not hypothesized to be able to perform such a distinction, since both eccentric and concentric hypertrophy can potentially influence the QRS-T angle. Due to the retrospective nature of the study, baseline data were not available for all cohorts. However, this does not affect the prognostic evaluation in the well-characterized Clinical-consecutive cohort. Finally, besides the most common conventional ECG criteria for LVH that we evaluated, other sets of criteria have also been acknowledged by the American Heart Association<sup>39</sup>, yet were not specifically studied.

## Conclusions

In conclusion, normal limits for the ECG-based spatial peaks QRS-T angle were defined using a large, healthy population. An increased QRS-T angle rarely occurred in health, was nearly always present in moderate or greater LVH, and was common even in patients without LVH but with cardiac co-morbidities. Increased QRS-T angle was also more accurate than conventional ECG criteria for detecting LVH. Based on the improved diagnostic and prognostic performance of the QRS-T angle compared to conventional ECG criteria for LVH, we propose that QRS-T angle should be investigated when ECGs are evaluated.

## Data availability

The datasets used and/or analyzed in current study are available from the corresponding author on reasonable request.

Received: 14 January 2022; Accepted: 14 July 2022

Published online: 06 September 2022

## References

- Dawson, A., Morris, A. D. & Struthers, A. D. The epidemiology of left ventricular hypertrophy in type 2 diabetes mellitus. *Diabetologia* **48**(10), 1971–1979 (2005).
- Shenasa, M. & Shenasa, H. Hypertension, left ventricular hypertrophy, and sudden cardiac death. *Int. J. Cardiol.* **237**, 60–63 (2017).
- Cuspidi, C., Rescaldani, M., Sala, C. & Grassi, G. Left-ventricular hypertrophy and obesity: A systematic review and meta-analysis of echocardiographic studies. *J. Hypertens.* **32**(1), 16–25 (2014).
- Narayanan, K. *et al.* Left ventricular diameter and risk stratification for sudden cardiac death. *J. Am. Heart Assoc.* **3**(5), e001193 (2014).
- Bacharova, L. & Estes, E. H. Left ventricular hypertrophy by the surface ECG. *J. Electrocardiol.* **50**(6), 906–908 (2017).
- Bacharova, L. Electrical and structural remodeling in left ventricular hypertrophy—A substrate for a decrease in QRS voltage?. *Ann. Noninvasive Electrocardiol.* **12**(3), 260–273 (2007).
- Reichek, N. & Devereux, R. B. Left ventricular hypertrophy: Relationship of anatomic, echocardiographic and electrocardiographic findings. *Circulation* **63**(6), 1391–1398 (1981).
- Maanja, M. *et al.* Diffuse myocardial fibrosis reduces electrocardiographic voltage measures of left ventricular hypertrophy independent of left ventricular mass. *J. Am. Heart Assoc.* **6**(1), e003795 (2017).
- Sundström, J. *et al.* Echocardiographic and electrocardiographic diagnoses of left ventricular hypertrophy predict mortality independently of each other in a population of elderly men. *Circulation* **103**(19), 2346–2351 (2001).
- Bacharova, L. *et al.* Changing role of ECG in the evaluation left ventricular hypertrophy. *J. Electrocardiol.* **45**(6), 609–611 (2012).
- Man, S. *et al.* Role of the vectorcardiogram-derived spatial QRS-T angle in diagnosing left ventricular hypertrophy. *J. Electrocardiol.* **45**(2), 154–160 (2012).
- Zhang, Z. M., Rautaharju, P. M., Prineas, R. J., Tereshchenko, L. & Soliman, E. Z. Electrocardiographic QRS-T angle and the risk of incident silent myocardial infarction in the Atherosclerosis Risk in Communities study. *J. Electrocardiol.* **50**(5), 661–666 (2017).
- Oehler, A., Feldman, T., Henrikson, C. A. & Tereshchenko, L. G. QRS-T angle: A review. *Ann Noninvasive Electrocardiol.* **19**(6), 534–542 (2014).
- Yamazaki, T., Froelicher, V. F., Myers, J., Chun, S. & Wang, P. Spatial QRS-T angle predicts cardiac death in a clinical population. *Heart Rhythm* **2**(1), 73–78 (2005).
- Schelbert, E. B. *et al.* Myocardial fibrosis quantified by extracellular volume is associated with subsequent hospitalization for heart failure, death, or both across the spectrum of ejection fraction and heart failure stage. *J. Am. Heart Assoc.* **4**(12), e002613 (2015).
- Schlegel, T. T. *et al.* Accuracy of advanced versus strictly conventional 12-lead ECG for detection and screening of coronary artery disease, left ventricular hypertrophy and left ventricular systolic dysfunction. *BMC Cardiovasc. Disord.* **10**, 28 (2010).
- Sokolow, M. & Lyon, T. P. The ventricular complex in left ventricular hypertrophy as obtained by unipolar precordial and limb leads. *Am. Heart J.* **37**(2), 161–186 (1949).
- Casale, P. N. *et al.* Electrocardiographic detection of left ventricular hypertrophy: Development and prospective validation of improved criteria. *J. Am. Coll. Cardiol.* **6**(3), 572–580 (1985).
- Molloy, T. J., Okin, P. M., Devereux, R. B. & Kligfield, P. Electrocardiographic detection of left ventricular hypertrophy by the simple QRS voltage-duration product. *J. Am. Coll. Cardiol.* **20**(5), 1180–1186 (1992).
- Willems, J. L. *et al.* Criteria for intraventricular conduction disturbances and pre-excitation. World Health Organization/International Society and Federation of Cardiology Task Force Ad Hoc. *J. Am. Coll. Cardiol.* **5**(6), 1261–1275 (1985).
- Kors, J. A., van Herpen, G., Sittig, A. C. & van Bommel, J. H. Reconstruction of the Frank vectorcardiogram from standard electrocardiographic leads: Diagnostic comparison of different methods. *Eur. Heart J.* **11**(12), 1083–1092 (1990).
- Cortez, D. L. & Schlegel, T. T. When deriving the spatial QRS-T angle from the 12-lead electrocardiogram, which transform is more Frank: Regression or inverse Dower?. *J. Electrocardiol.* **43**(4), 302–309 (2010).
- Lang, R. M. *et al.* Recommendations for chamber quantification: A report from the American Society of Echocardiography's Guidelines and Standards Committee and the Chamber Quantification Writing Group, developed in conjunction with the European Association of Echocardiography, a branch of the European Society of Cardiology. *J. Am. Soc. Echocardiogr.* **18**(12), 1440–1463 (2005).
- Maceira, A. M., Prasad, S. K., Khan, M. & Pennell, D. J. Normalized left ventricular systolic and diastolic function by steady state free precession cardiovascular magnetic resonance. *J. Cardiovasc. Magn. Reson.* **8**(3), 417–426 (2006).

25. Schelbert, E. B. *et al.* Temporal relation between myocardial fibrosis and heart failure with preserved ejection fraction: Association with baseline disease severity and subsequent outcome. *JAMA Cardiol.* **2**(9), 995–1006 (2017).
26. Pencina, M. J., D'Agostino, R. B. & Vasan, R. S. Evaluating the added predictive ability of a new marker: From area under the ROC curve to reclassification and beyond. *Stat. Med.* **27**(2), 157–172 (2008) (**discussion 207–212**).
27. Voulgari, C., Pagoni, S., Tesfaye, S. & Tentolouris, N. The spatial QRS-T angle: Implications in clinical practice. *Curr. Cardiol. Rev.* **9**(3), 197–210 (2013).
28. Devereux, R. B. & Reichek, N. Repolarization abnormalities of left ventricular hypertrophy. Clinical, echocardiographic and hemodynamic correlates. *J. Electrocardiol.* **15**(1), 47–53 (1982).
29. Bacharova, L. *et al.* Second statement of the working group on electrocardiographic diagnosis of left ventricular hypertrophy. *J. Electrocardiol.* **44**(5), 568–570 (2011).
30. Tanriverdi, Z., Besli, F., Gungoren, F. & Tascanov, M. B. What is the normal range of the frontal QRS-T angle?. *Diabetes Res. Clin. Pract.* **160**, 107645 (2020).
31. Kors, J. A. *et al.* Spatial QRS-T angle as a risk indicator of cardiac death in an elderly population. *J. Electrocardiol.* **36**(Suppl), 113–114 (2003).
32. Rautaharju, P. M., Kooperberg, C., Larson, J. C. & LaCroix, A. Electrocardiographic predictors of incident congestive heart failure and all-cause mortality in postmenopausal women: The Women's Health Initiative. *Circulation* **113**(4), 481–489 (2006).
33. Lipton, J. A. *et al.* Abnormal spatial QRS-T angle predicts mortality in patients undergoing dobutamine stress echocardiography for suspected coronary artery disease. *Coron. Artery Dis.* **21**(1), 26–32 (2010).
34. Kenttä, T. *et al.* QRS-T morphology measured from exercise electrocardiogram as a predictor of cardiac mortality. *Europace* **13**(5), 701–707 (2011).
35. Dilaveris, P. *et al.* The spatial QRS-T angle as a marker of ventricular repolarisation in hypertension. *J. Hum. Hypertens.* **15**(1), 63–70 (2001).
36. Voulgari, C. *et al.* Spatial QRS-T angle: Association with diabetes and left ventricular performance. *Eur. J. Clin. Invest.* **36**(9), 608–613 (2006).
37. Cortez, D., Sharma, N., Devers, C., Devers, E. & Schlegel, T. T. Visual transform applications for estimating the spatial QRS-T angle from the conventional 12-lead ECG: Kors is still most Frank. *J. Electrocardiol.* **47**(1), 12–19 (2014).
38. Benjamin, E. J. *et al.* Impact of atrial fibrillation on the risk of death: The Framingham Heart Study. *Circulation* **98**(10), 946–952 (1998).
39. Bacharova, L. & Ugander, M. Left ventricular hypertrophy: The relationship between the electrocardiogram and cardiovascular magnetic resonance imaging. *Ann. Noninvasive Electrocardiol.* **19**(6), 524–533 (2014).

### Author contributions

M.M., T.S., R.K. and M.U. designed the study and drafted the manuscript. M.M., T.W. and E.S. participated in study design and CMR data acquisition and analysis. M.M., T.S., L.B. and M.U. participated in ECG data analysis. M.M., T.S. and M.U. performed statistical analysis. All authors have read and approved the final manuscript.

### Funding

Open access funding provided by Karolinska Institute. This work was supported in part by Grants from the Swedish Research Council, Swedish Heart and Lung Foundation, Stockholm County Council, and Karolinska Institutet.

### Competing interests

Dr. Schlegel is a principal of Nicollier-Schlegel SARL, a company that performs ECG research consultancy using the software used in the present study. Dr. Ugander reports non-financial support from Siemens Healthcare outside the submitted work. The other authors have nothing to disclose.

### Additional information

**Correspondence** and requests for materials should be addressed to M.U.

**Reprints and permissions information** is available at [www.nature.com/reprints](http://www.nature.com/reprints).

**Publisher's note** Springer Nature remains neutral with regard to jurisdictional claims in published maps and institutional affiliations.



**Open Access** This article is licensed under a Creative Commons Attribution 4.0 International License, which permits use, sharing, adaptation, distribution and reproduction in any medium or format, as long as you give appropriate credit to the original author(s) and the source, provide a link to the Creative Commons licence, and indicate if changes were made. The images or other third party material in this article are included in the article's Creative Commons licence, unless indicated otherwise in a credit line to the material. If material is not included in the article's Creative Commons licence and your intended use is not permitted by statutory regulation or exceeds the permitted use, you will need to obtain permission directly from the copyright holder. To view a copy of this licence, visit <http://creativecommons.org/licenses/by/4.0/>.

© The Author(s) 2022